AA12 | PSTR039.09

Quantifying uncertainty of parameter estimates when applying drift diffusion models to temporally-dependent decision data

Gabriel Riegner[1], Pamela Reinagel[2], Armin Schwartzman[1]
[1]Halıcıoğlu Data Science Institute, UCSD | [2]Department of Neurobiology, UCSD
UC San Diego

Abstract

Decision behavior changes over time, exhibiting temporal correlations and non-stationarity. Existing Drift Diffusion Model (DDM) fitting methods rely on restrictive assumptions that decisions are independent and parameters are constant over time.

To address these limitations, we propose a computationally efficient method for estimating analytical uncertainties in DDM parameters that are robust to unmodeled parameter variability and temporal correlations between trials.

We apply this method to choice and reaction-time data from rats in a visual decision task, allowing us to resolve non-stationary shifts in decision-making parameters across different timescales. This work establishes a robust method for studying dynamic decision processes in naturalistic experiments by relaxing assumptions of correct specification and trial independence.

Introduction

A. Two-Alternative Forced Choice (2AFC) B. Psychometric Function C. Chronometric Function

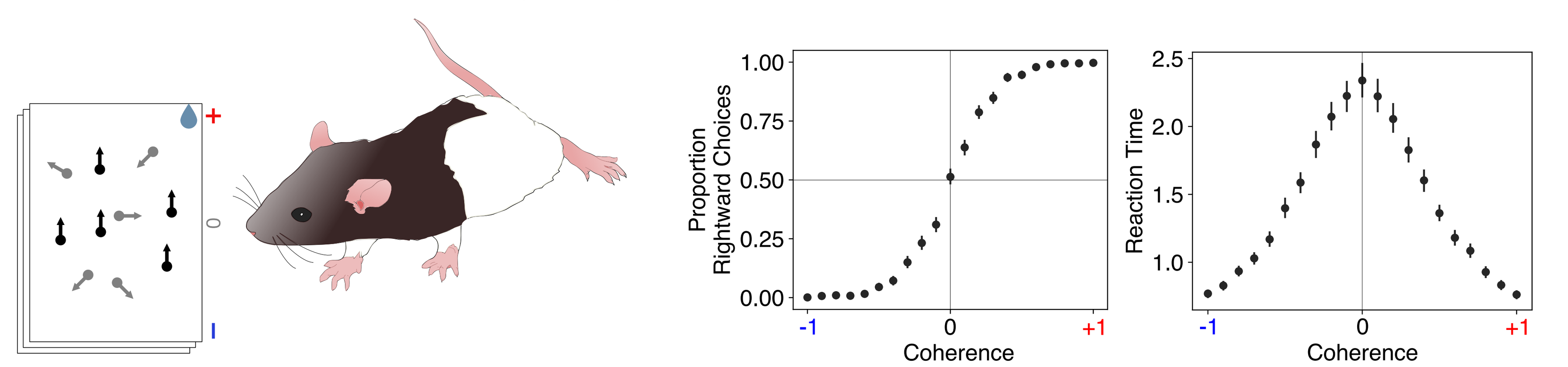

Figure 1: Choice and Reaction Times Change with Coherence.

(A) Rats decide whether random-dot motion moves left (-) or right (+) based on motion coherence, with correct choices rewarded by access to water. (B/C) Simulated choice and reaction time functions of motion coherence under the drift diffusion model (described below). (B) The proportion of rightward choices increases with increasing rightward coherence. (C) Reaction times decrease with increasing motion coherence magnitude.

A. Choice and Reaction Times Fit by Day B. Choice and Reaction Times Fit by Trial in Day

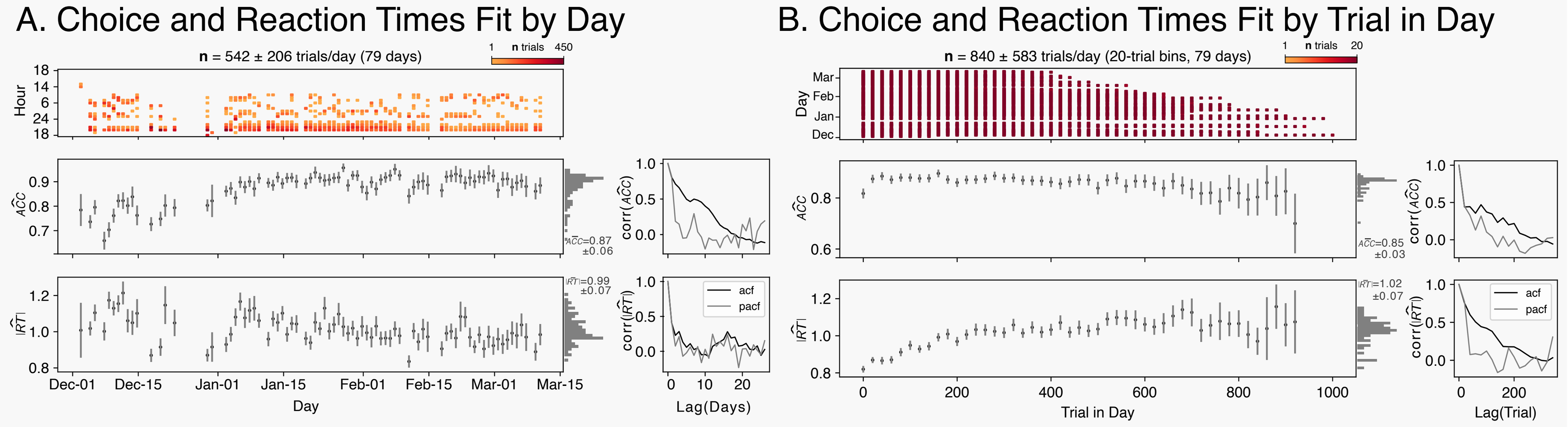

Figure 2: Choice and Reaction Times Change Over Time. Dataset from (Reinagel 2013).

(A) and (B) show trials from a single rat from 79 days of fixed motion coherence. Error bars show +/-2 standard errors assuming *iid* trials. **Row 1** shows the number of trials in (A) per hour grouped by day and in (B) per day grouped by trial in day. **Row 2** shows choice accuracy and its autocorrelation, and **Row 3** shows reaction time and its autocorrelation.

Drift Diffusion Model (DDM)

Parameters of the DDM

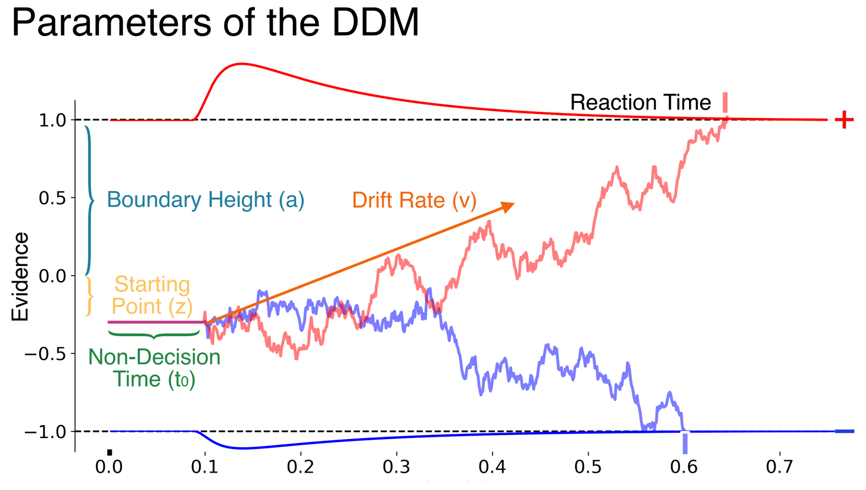

Figure 3: Choice and Reaction Times under the DDM.

The DDM models a decision as the accumulations of noisy evidence over time toward one of two (+/-) choice boundaries. Starting Point (z) indicates an initial bias toward one of the two choices. Non-Decision Time (t_0) accounts for perceptual and motor processes unrelated to evidence accumulation. Drift Rate (v) reflects the average speed and direction of evidence accumulation. Boundary Height (a) represents the amount of evidence required to make a decision.

Point Estimation of DDM Parameters

A. Example Probability Function (Eq 4) B. Example Log-Likelihood Function (Eq 5)

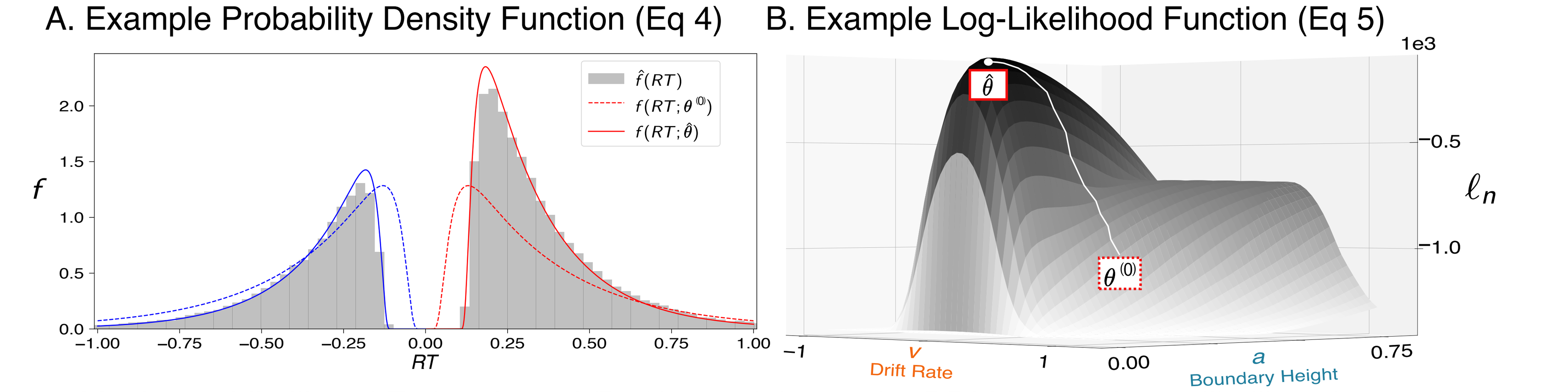

Figure 4: Maximum Likelihood Estimation. (A/B) Shows fitting of the DDM by maximum likelihood.

Notation:

Drift Diffusion Process

$$\text{(1)}\quad Z_\tau = az + \sum_{t=1}^{\tau} e_t, \quad e_t \sim \mathcal{N}(v\Delta\tau, \sigma^2\Delta\tau)$$

boundary height (a); relative starting point (z); Gaussian noise variance (σ^2); drift rate (v); diffusion time index with resolution $\Delta\tau$

Choice and Reaction Time for a Single Trial

$$\text{(2)}\quad RT = \begin{cases} +\{\tau > 0 : Z_\tau \geq +a\}\cdot\Delta\tau + t_0 \\ -\{\tau > 0 : Z_\tau \leq -a\}\cdot\Delta\tau - t_0 \end{cases}$$

upper boundary crossing; lower boundary crossing; non-decision time (t_0)

$\mathrm{sign}(RT)$ is the binary choice and $|RT|$ is the reaction time

Choices and Reaction Times for Multiple Trials

$$\text{(3)}\quad \{RT_i\}_{i=1}^{n} \sim f(RT; \boldsymbol{\theta} = (a, t_0, v, z))$$

joint choice and reaction time distribution; trial index

Point Estimation:

Probability Density Function

(Feller, 1968; Navarro and Fuss, 2009)

$$\text{(4)}\quad f(RT;\theta) = \frac{4\pi}{a^2}\exp\left(\frac{\mathrm{sign}(RT)avw - v^2(|RT|-t_0)}{2}\right) \times \sum_{k=1}^{\infty} k\exp\left(-\frac{2k^2\pi^2(|RT|-t_0)}{a^2}\right)\sin(k\pi w)$$

$|RT| > t_0$, $\quad w = \frac{1-\mathrm{sign}(RT)z}{2}$

Log Likelihood Function

$$\text{(5)}\quad \ell_n(\theta; \{RT_i\}_{i=1}^{n}) = \frac{1}{n}\sum_{i=1}^{n}\log f(RT_i;\theta)$$

average log-likelihood over n trials

Maximum Likelihood Estimator

$$\text{(6)}\quad \hat{\theta} = \operatorname*{argmax}_{\theta}\ \ell_n(\theta; \{RT_i\}_{i=1}^{n})$$

Objective: Quantify uncertainty of DDM parameters robust to unmodeled temporal variability and correlations across trials.

Uncertainty Estimation of DDM Parameters

Covariance Estimation:

Hessian Matrix

$$\text{(7)}\quad \widehat{\mathscr{H}} = -\frac{1}{n}\sum_{i=1}^{n}\frac{\partial^2}{\partial\theta\partial\theta'}\log f(RT_i;\hat{\theta}) = -\frac{1}{n}\frac{\partial^2}{\partial\theta\partial\theta'}\ell_n(\hat{\theta})$$

matrix of second derivatives of the log-likelihood

Fisher Information Matrix

$$\text{(8)}\quad \widehat{\mathscr{I}} = \frac{1}{n}\sum_{i=1}^{n}\left(\frac{\partial}{\partial\theta}\log f(RT_i;\hat{\theta})\right)\left(\frac{\partial}{\partial\theta}\log f(RT_i;\hat{\theta})\right)' = \frac{1}{n}\sum_{i=1}^{n}\hat{S}_i\hat{S}_i'$$

matrix of outer products of the score vectors for each trial i

Sample Hessian

$$\text{(9)}\quad \widehat{V}_{\mathrm{SH}} = \widehat{\mathscr{H}}^{-1}$$

Outer Product

$$\text{(10)}\quad \widehat{V}_{\mathrm{OP}} = \widehat{\mathscr{I}}^{-1}$$

Misspecification Robust $\mathscr{I} \neq \mathscr{H}$

$$\text{(11)}\quad \widehat{V}_{\mathrm{MR}} = \widehat{\mathscr{H}}_\theta^{-1}\widehat{\mathscr{I}}_\theta\widehat{\mathscr{H}}_\theta^{-1}$$

Autocorrelation Robust

$$\text{(12)}\quad \widehat{V}_{\mathrm{AR}} = \widehat{\mathscr{H}}^{-1}\left(\frac{1}{n}\sum_{i,j=1}^{n} w_{|i-j|}\hat{S}_i\hat{S}_j'\right)\widehat{\mathscr{H}}^{-1}$$

weights that taper long-range autocorrelations

A. Convergence B. Uncertainty

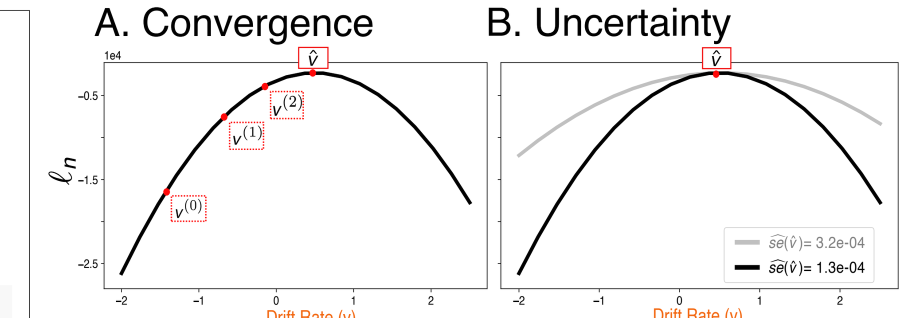

Figure 5: Hessian Matrix. (A) Shows convergence speed, (B) shows uncertainty/Fisher Information.

Theoretical Properties:

Consistent Estimation under *Ergodicity*
(Hansen 2022b, Theorem 10.8) (Hansen 2022a, Theorem 14.9)

$$\text{(13)}\quad \hat{\theta} \xrightarrow[p]{} \theta_0 \text{ as } n \to \infty$$

Asymptotic Normality under *Strong Mixing*
(Hansen 2022b, Theorem 10.16) (Hansen 2022a, Theorem 14.15)

$$\text{(14)}\quad \sqrt{n}(\hat{\theta} - \theta_0) \xrightarrow[d]{} \mathcal{N}(0, V) \text{ as } n \to \infty$$

Validation by Simulation

A/B. Correctly Specified Model C/D. Misspecified Parameter Variability

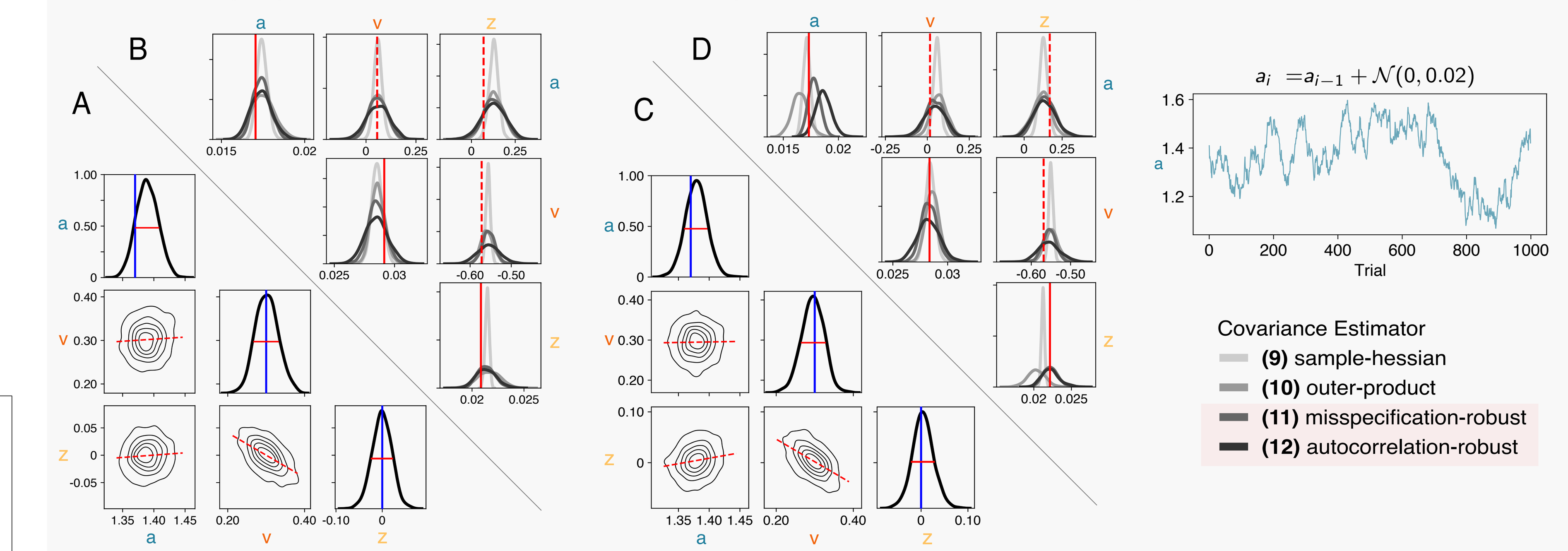

Figure 6: Point and Uncertainty Estimation Performance.

Choice and reaction time data were simulated from equation **(3)**, with n=1000 trials and b=900 repeats. **(A/B)** is a setting with constant parameters from trial-to-trial, while **(C/D)** adds autoregressive variability to the boundary height (a). **(A/C)** shows point estimates as density curves relative to their true parameters (a=1.37, v=0.3, z=0) and **(C/D)** shows uncertainty estimates relative to their empirically true values.

Data Analysis Results

A. DDM Parameters Fit by Day B. DDM Parameters Fit by Trial in Day

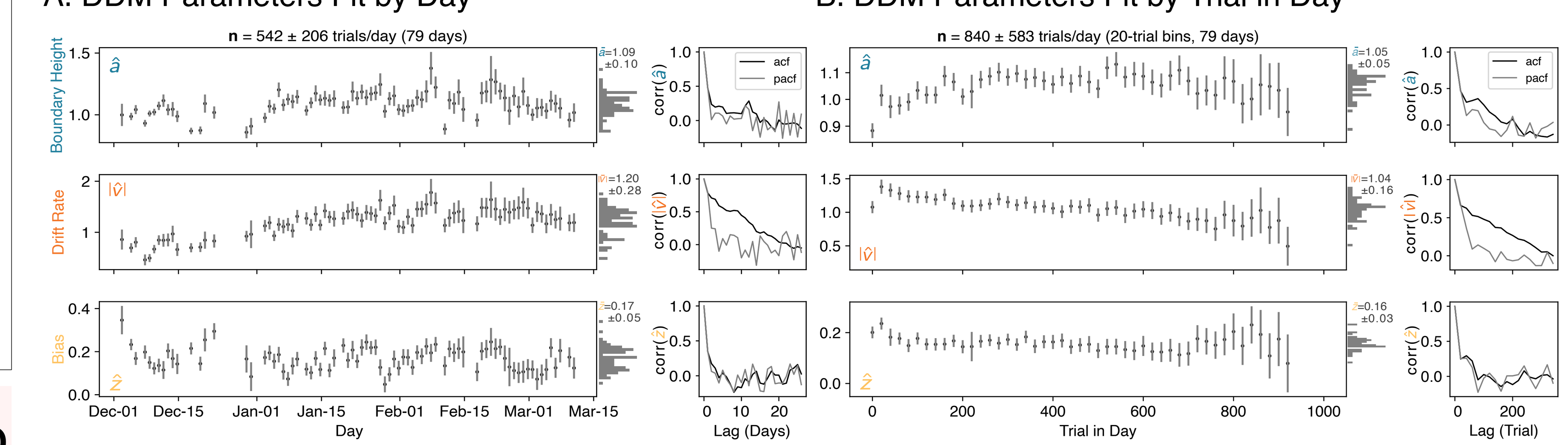

Figure 7: DDM Parameters Change Over Time.

Fits to rat behavioral data from **Figure 2**. **(A)** and **(B)** show non-stationary shifts in decision-making parameters relative to their uncertainties across different timescales, where **(A)** shows changes over days and **(B)** shows changes over trials within day. Error bars show +/- 2 standard errors calculated from equation **(12)** for robustness to unmodeled temporal variability and autocorrelation. **Rows 1-3** show estimates of boundary height (a), absolute drift rate (v), and starting bias (z) and their autocorrelations.

Conclusions

- DDM parameters and their uncertainties can be reliably estimated despite the presence of unmodeled temporal variability and correlations across trials.
- Applying this approach to rat decision-making data reveals temporal variations in the underlying decision parameters across different timescales.
- The Hessian matrix enables efficient point estimates and uncertainty intervals for thousands of trials, improving computation speed compared to existing methods.

References

Feller, W. (1968). *An introduction to probability theory and its applications* (3rd rev. ed.). Wiley.
Hansen, B. E. (2022a). *Econometrics*. Princeton University Press.
Hansen, B. E. (2022b). *Probability and statistics for economists*. Princeton University Press.
Navarro, D. J., & Fuss, I. G. (2009). Fast and accurate calculations for first-passage times in Wiener diffusion models. *Journal of Mathematical Psychology*, 53(4), 222–230.
Reinagel, P. (2013). Speed and Accuracy of Visual Motion Discrimination by Rats. *PLoS ONE*, 8(6), e68505.

Link to Poster

Acknowledgements

National Institutes of Health
The BRAIN Initiative

NIH/NINDS (1R34NS132037-0) BRAIN Initiative Grant.

gariegner@ucsd.edu